Development of crane-mounted hyperspectral imagery system for stable analysis of paddy field

Yohei Minekawa, Kuniaki Uto, Yukio Kosugi
Interdisciplinary Graduate School of Science and Engineering Tokyo Institute of Technology
G2-16, 4259, Nagatsuta, Midori-ku, Yokohama, Kanagawa 226-8502, Japan
{m02minekawa, uto, kosugi}@pms.titech.ac.jp

Kunio Oda
Yamagata Prefectural Agricultural Experiment Station Shonai Branch Technology of Paddy Farming
25, Yamanomae, Fujishima, Fujishima-cho, Higashitagawa-gun, Yamagata 999-7601, Japan
odaku@pref.yamagata.jp

Abstract: We proposed a new system to collect hyperspectral data using a general cargo crane. The system has advantageous characteristics for precise data collection and analysis. In order to evaluate the validity, we performed the system on actual rice paddy field and analyzed the observed data. On the process, we could successfully extract the pure vegetation spectrum with high stability.

The data taken by the system are useful for detail analysis among fields. In future development, it can be used for obtaining the grand truth for calibrating satellite or aerial hyperspectral images.

Keywords: spectroscopy, rice paddy, crane, hyperspectral, NDVI, salt air damage.

1. Introduction

In recent years, hyperspectral data became of great importance for agricultural fields. The data contain a lot of beneficial information which cannot be observed through our low-resolution RGB system of the eyes directly. For example, there are reports which suggest that one of the ingredient contents of fruits is related with some part of hyperspectral data [1].

Those data can be used for the control of fields in particular for quality control of crops. For example, they are used for extracting the distribution of crops and growth stages, analyzing crop's damages from disease or harmful insects and finding appropriate timing for fertilizers. In order to evaluate over huge agricultural lands practically, hyperspectral remote sensing is a useful tool especially when satellite or aerial images are well calibrated by the ground truth data.

However, there are still some discussions about the way to obtain hyperspectral ground truth data. Conventionally, the ground truth data were mostly collected by wide angle spectrometers which gather averaged reflectance data with respect to some crops. In the wide angle measurement, without using imaging systems, it is difficult to obtain pure spectrum with respect to each part of a crop. If we use narrower angle reflectance sensor, it might be a tedious work to gather the spectral data over a certain area of a field. In order to overcome these problems, we designed a new system for gathering hyperspectral data using a general cargo crane as a low-altitude data acquisition system.

2. Hyperspectral data acquisition system using a cargo crane

Fig.1 shows the diagram of the system. The system is mounted on the tip of the crane, and consists of a hyperspectral line sensor and battery-powered PC for data storage. They are controlled remotely from another PC on the ground. The line spectrometer consists of a Prism-Grating-Prism type spectrograph and 2/3" CCD camera with effective pixels 754 (in wavelength axis) x 484 (in special axis). Therefore, the number of pixels in spatial axis is 484 and the maximum number of pixels in wavelength axis is 754. The sensor can take spectrum of every 5nm wavelength between 400nm and 1000nm in each pixel.

Fig.2 (a) is the illustration of the cargo crane seen from rear side, and Fig.2 (b) is that from upper side while in the operation. The crane arm can be rotated horizontally to observe the field (Fig.2 b). The crane posture alpha can be also changed to adjust the range and spot for the image (Fig.2 a).

The hyperspectral data collected by the system are converted to reflectance data using the standard white board data collected in the same time. After the transformation, pseudo-color images are created using the reflectance at R (650nm), G (550nm) and B (450nm) in each pixel.

Fig.3 (a) is the photograph at actual experiment, and (b) is the detailed view of the sensor.

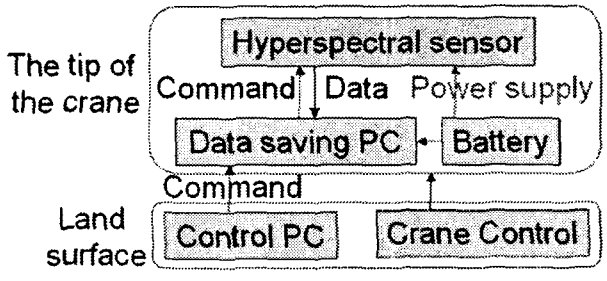

Fig. 1. The diagram of the system.

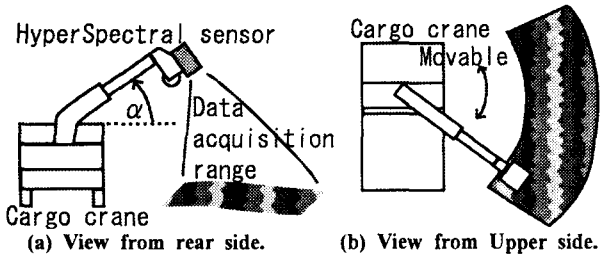

(a) View from rear side. (b) View from Upper side.

Fig. 2. The illustration of the cargo crane.

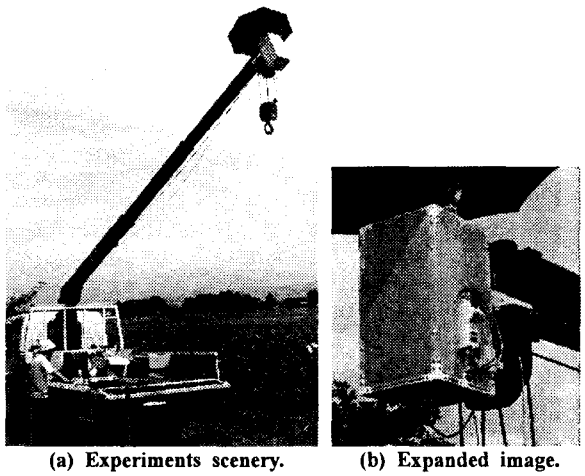

(a) Experiments scenery. (b) Expanded image.

Fig. 3. The actual experiments scenery.

3. Data classification

The data collected by the system contain not only targeted vegetation data, but also in non-vegetation, mixel and shadow areas. It is necessary to sort out these areas in the preprocessing to extract pure spectrum of the vegetation part.

1) Classification of vegetation and non-vegetation area

The hyperspectral data in vegetation areas have specific tendency that contain high reflectance in near-infrared wavelengths. In order to sort out the non-vegetation area, NDVI (Normalized Difference Vegetation Index) that is shown in following equation, is commonly used.

$$NDVI = \frac{IR - R}{IR + R}. \quad (1)$$

Where, IR is the mean reflectance in near-infrared wavelengths (770 to 870nm) and R is that in red wavelengths (650 to 670nm). NDVI values are calculated in each pixel.

The NDVI value in vegetation area is high, whereas that in non-vegetation area takes low. Therefore, the threshold method is appropriate for the separation.

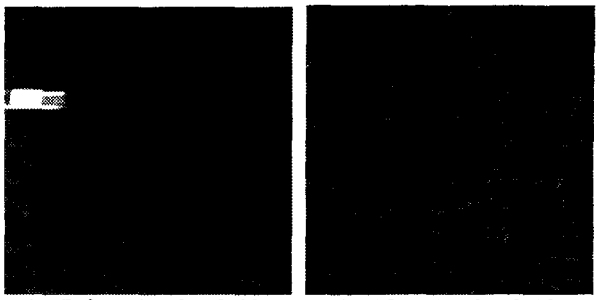

(a) Before the threshold (b) After the threshold

Fig. 4. Pseudo-color images of hyperspectral data before and after the threshold (NDVI>=0.6).

Fig.4 (a) is the pseudo-color image of hyperspectral data before the threshold and (b) is that after the threshold operation. According to the preliminary results, the vegetation areas are successfully categorized automatically.

2) Classification of leaf and ear

About 1 month before harvest time, rice come into ear. There is much difference in spectra between leaves and ears. Therefore, it is necessary to categorize the leaf and ear part to have pure spectra.

Fig.5 shows the distribution for leaf, ear, mixel and shadow area plotted against NDVI and mean reflectance in near-infrared wavelengths (770 to 870nm). These samples are categorized and extracted by hand. According to Fig.5, the data in each category are clustering around specific points. Therefore, the categorizations can be made by threshold operation. The conditions for threshold are shown in Table.1.

Fig.6 (a) is the pseudo-color image about 1 month before the harvest time. Fig.6 (b) is the mask image for leaf and (c) is that for ear by the threshold. According to Fig.6, these areas are successfully categorized automatically.

4. The difference among the posture

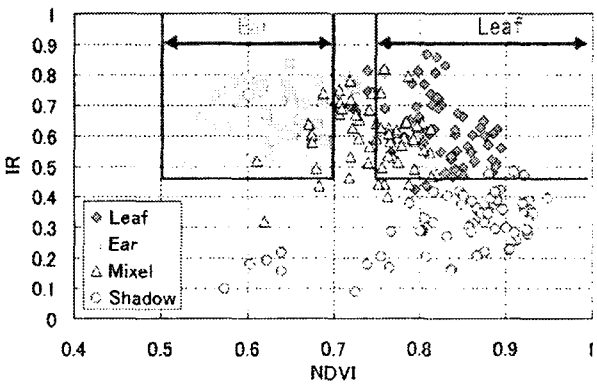

Fig. 5. The distribution of data in each category against NDVI and mean reflectance in near-infrared (770 to 870nm).

Table 1. The threshold conditions between leaf and ear.

	Leaf	Ear
NDVI	0.75 – 1.00	0.50 – 0.70
IR	>=0.45	>=0.45

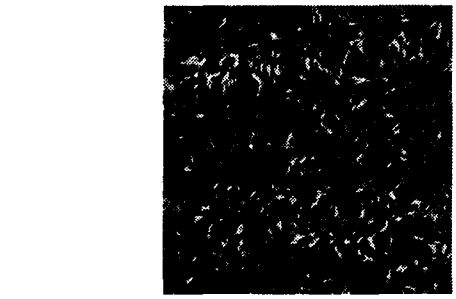

(a) Before the classification

(b) Leaf mask image

(c) Ear mask image

Fig. 6. Pseudo-color images of hyperspectral data before and after the classification.

The system has flexibility for the range and spot for data collection by changing the crane arm posture (Fig.2 a). However, there comes one question about the comparability among the data that are taken in different conditions. In order to answer the question, we compared the mean spectra that are taken in different crane postures in the same agricultural land. Ideally, the spectra should be taken by close distance and from above of the subject. Therefore, the mean data taken with alpha = 0 deg are used as the criterion data.

Fig.7 (a), (b) show the error ratio in near-infrared wavelengths (850 to 900nm) of leaf and ear. In this case, the error means the difference between criterion spectra and the spectra taken in other conditions.

According to Fig.7, the data taken in difference conditions are possible to compare except for the condition of a high data acquisition angle.

5. Preliminary observation of typhoon damages

We took the hyperspectral data about the rice paddy that had suffered from salt damages due to the typhoon 0415, Megi, in 2004, in Yamagata pref. of Japan. According to the analyses of these data, two indexes that can be used for the damage evaluation are extracted.

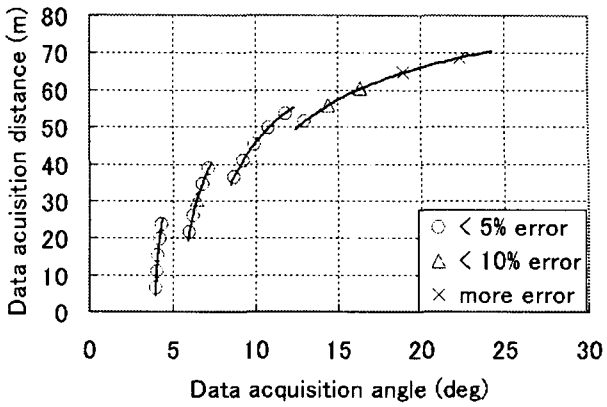

(a) The error ratio of leaf in different condition.

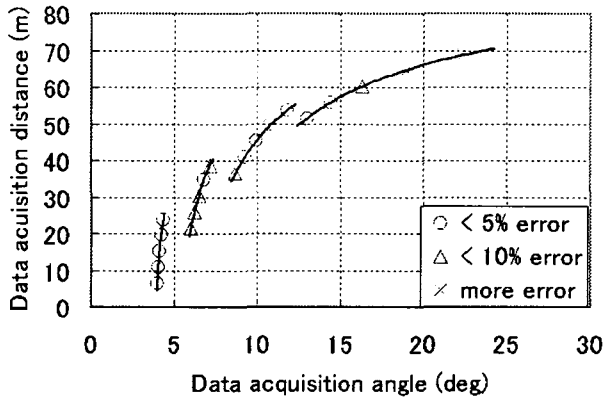

(b) The error ratio of ear in different condition.

Fig. 7. The error ratio in IR wave lengths between the data taken in the alpha = 0 deg condition and that in other conditions.

They are shown in equation (2).

$$\begin{cases} Index1 = LR(900) - LR(850) \\ Index2 = \{LR(550) - ER(550)\} \\ \qquad\quad -\{LR(500) - ER(500)\} \end{cases} \quad (2)$$

Where, LR(x) is the leaf's reflectance in the wavelength x nm, and ER(x) is the ear's reflectance in the wavelength x nm.

Fig. 8 shows the data plot against these indexes. According to Fig.8, the data are clearly separated in term of the intensity of damages, where the degrees of damages were manually examined.

6. Conclusions

We developed the hyperspectral data acquisition system using a general cargo crane. The system successfully worked for collecting hyperspectral data with high stability. In addition, using the classification technique, the data can be analyzed precisely to extract pure spectra in each agricultural land. The pure spectral data are useful as the grand truth when using satellite or aerial observations.

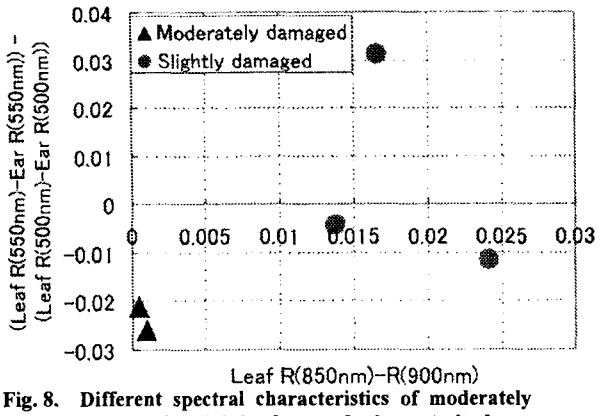

Fig. 8. Different spectral characteristics of moderately damaged and only slightly damaged plants (salt damages due to the typhoon 0415, Megi, in 2004, in Yamagata pref. of Japan).

References

[1] Mizuki Tsuta, Junichi Sugiyama and Yasuyuki Sagara, 2002.Near-Infrared Imaging Spectroscopy Based on Sugar Absorption Band for Melons, *Agric. Food Chem, Vol.50, pp.48-52.*